Transactions of the Korean Nuclear Society Spring Meeting
Jeju, Korea, May 7-8, 2026

Convergence Analysis of Various Coarse-Mesh Finite Difference (CMFD) Schemes in Fixed-Source and Eigenvalue Neutron Transport Problems

Taesuk Oh [a*], Ben Lindley [a]
[a] *University of Wisconsin-Madison, Madison, WI, USA*
Department of Nuclear Engineering and Engineering Physics
[*] *Corresponding author: toh8@wisc.edu*

Keywords : Coarse-Mesh Finite Difference (CMFD), Convergence Analysis, Fixed-Source, Neutron Transport

1. Introduction

The coarse-mesh finite difference (CMFD) method has been widely employed as an acceleration technique for iterative neutron transport calculations [1]. The method embeds correction factors within a low-order finite difference method (FDM) framework so that the coarse-mesh balance preserves the neutron current of the reference high-order solution, thereby retaining transport-level accuracy while benefiting from the computational efficiency of FDM.

Based on this current-preserving principle, several CMFD variants have been developed. Partial-current CMFD (pCMFD) modifies the treatment of surface currents [2], while one-node CMFD restructures the correction factors to enable node-wise formulation and parallel execution [3]. The one-node structure has further motivated the development of Hybrid CMFD (HCMFD), where global and local acceleration levels are combined for efficient pin-wise nodal analysis [4,5]. In addition, alternative formulations such as lp-CMFD have been proposed to improve numerical stability [6].

The convergence behavior and stability characteristics of CMFD-type accelerations have been investigated in previous studies, particularly for conventional CMFD and pCMFD in both fixed-source and eigenvalue problems [7,8]. For one-node formulations, however, convergence analyses have primarily focused on fixed-source settings [9]. A comparative assessment that considers multiple CMFD variants simultaneously for both fixed-source and eigenvalue transport problems is therefore warranted. In this work, the convergence behavior of various CMFD schemes is systematically examined and compared for fixed-source and eigenvalue neutron transport problems.

2. CMFD Acceleration Schemes

Balance for neutron flux within a node of interest i as illustrated in Fig. 1 can be expressed as below:

$$\bar{J}_{i,i+1} - \bar{J}_{i-1,i} + \Sigma_{ri}\Delta x_i \bar{\phi}_i = \frac{\chi_{g,i}}{k}\sum_{g} \nu\Sigma_{fi}\Delta x_i \bar{\phi}_i, \quad (1)$$

where $\bar{J}_{i,i+1}$ denotes the net neutron current egressing from node i toward the consecutive node i+1, k is the multiplication factor, and all the other notations are that

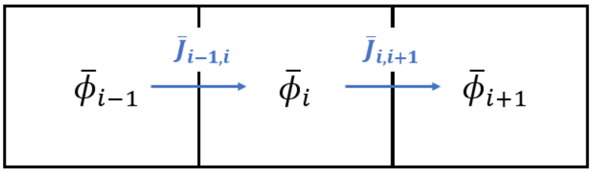

Fig. 1. Balance within a node of interest (from [10]).

of the convention. Exploiting diffusion theory, and approximating the gradient of flux to be linear, one gets

$$\bar{J}_{i,i+1} = -\widetilde{D}_{i,i+1}(\bar{\phi}_{i+1} - \bar{\phi}_i), \quad (2)$$

$$\widetilde{D}_{i,i+1} = \frac{2\left(\frac{D_i}{\Delta x_i}\right)\left(\frac{D_{i+1}}{\Delta x_{i+1}}\right)}{\frac{D_i}{\Delta x_i} + \frac{D_{i+1}}{\Delta x_{i+1}}}, \quad (3)$$

which is known as the finite difference method (FDM).

Correction factor $\widehat{D}_{i,i+1}$ is introduced to adjust the current to be that of the reference:

$$\bar{J}^{ref}_{i,i+1} = -\widetilde{D}_{i,i+1}(\bar{\phi}_{i+1} - \bar{\phi}_i) - \widehat{D}_{i,i+1}(\bar{\phi}_{i+1} + \bar{\phi}_i), \quad (4)$$

$$\widehat{D}_{i,i+1} = \frac{-\widetilde{D}_{i,i+1}(\bar{\phi}_{i+1} - \bar{\phi}_i) - \bar{J}^{ref}_{i,i+1}}{(\bar{\phi}_{i+1} + \bar{\phi}_i)}. \quad (5)$$

The neutron balance equation, i.e., Eq. (1), is a well-defined problem. Therefore, by correcting the net current through Eqs. (4) and (5) within a low-order FDM formulation, the coarse-mesh scheme becomes equivalent to the reference high-order solution, regardless of the spatial mesh size employed [1]. As a result, a higher-order solution, i.e., reference solution, can be obtained through an accelerated procedure that retains the computational efficiency of the FDM method, which forms the basis of the coarse-mesh finite difference (CMFD) approach.

Several variants of CMFD have been proposed. Among the earliest and most widely adopted is the partial-current CMFD (pCMFD), which preserves partial currents rather than directly correcting the net current [2]. Since the net current is defined as the difference between outgoing and incoming partial currents, its preservation follows naturally. This formulation provides markedly improved numerical stability compared to conventional CMFD. The partial-current form is given in Eqs. (6) and (7), where $\widehat{D}^{+}_{i,i+1}$ appears in Eq. (6) and $\widehat{D}^{-}_{i,i+1}$ appears in Eq. (7), corresponding to the outgoing and incoming partial currents, respectively.

$$\bar{J}^{+ref}_{i,i+1} = -\frac{\widetilde{D}_{i,i+1}(\bar{\phi}_{i+1} - \bar{\phi}_i) + 2\widehat{D}^{+}_{i,i+1}\bar{\phi}_i}{2}, \quad (6)$$

$$\bar{J}^{-ref}_{i,i+1} = \frac{\widetilde{D}_{i,i+1}(\bar{\phi}_{i+1} - \bar{\phi}_i) + 2\widehat{D}^{-}_{i,i+1}\bar{\phi}_{i+1}}{2}. \quad (7)$$

The one-node CMFD introduces correction factors separately for each node, which is inherently favorable for parallel implementation [3]. Equations (8) and (9) represent the net current at each node using a common surface flux $\bar{\phi}_s$.

$$\bar{J}_{i,i+1} = -\frac{2D_i}{\Delta x_i}(\bar{\phi}_s - \bar{\phi}_i) - \frac{2\widehat{D}^R_i}{\Delta x_i}(\bar{\phi}_s + \bar{\phi}_i), \quad (8)$$

$$\bar{J}_{i,i+1} = -\frac{2D_{i+1}}{\Delta x_{i+1}}(\bar{\phi}_{i+1} - \bar{\phi}_s) - \frac{2\widehat{D}^L_{i+1}}{\Delta x_{i+1}}(\bar{\phi}_s + \bar{\phi}_{i+1}). \quad (9)$$

It is noted that node i updates its current information without requiring information from node $i+1$. By equating Eqs. (8) and (9), an expression for the surface flux $\bar{\phi}_s$ is obtained, and after algebraic manipulation, the correction factors are given as follows:

$$\widehat{D}^R_i = -\frac{\Delta x_i \bar{J}^{ref}_{i,i+1} + 2D_i(\bar{\phi}^{ref}_s - \bar{\phi}_i)}{2(\bar{\phi}^{ref}_s + \bar{\phi}_i)}, \quad (10)$$

$$\widehat{D}^L_{i+1} = -\frac{\Delta x_{i+1} \bar{J}^{ref}_{i,i+1} + 2D_{i+1}(\bar{\phi}_{i+1} - \bar{\phi}^{ref}_s)}{2(\bar{\phi}^{ref}_s + \bar{\phi}_{i+1})}. \quad (11)$$

The correction factors introduced here have units of [cm], unlike those in the conventional CMFD schemes discussed earlier. Although originally developed to facilitate parallel acceleration, the one-node CMFD can be applied in a manner analogous to conventional CMFD, preserving the net current across two contiguous nodes, i.e., in a two-node scheme. Further details can be found in [9,10].

In a similar manner, the pCMFD scheme can be implemented within a parallel framework, commonly referred to as one-node pCMFD. For a given node, incoming partial currents at each boundary are prescribed as boundary conditions. A local higher-order fixed-source problem is then solved to update the node-wise flux and outgoing partial currents. The updated outgoing partial currents subsequently serve as boundary conditions for neighboring nodes. A detailed description of the one-node formulations can be found in [9]. The lp-CMFD scheme is not considered in this work.

3. Numerical Results

Figure 2 illustrates the one-dimensional one-group slab problem with a uniform fixed source distribution [7]. The transport equation was discretized using the discrete ordinates method with S_{16} angular quadrature throughout this work [11].

Table 1 summarizes the number of iterations required for each method. Here, SI denotes source iteration without acceleration. The coarse-mesh rebalance (CMR) method was also included for comparison [11]. All methods produced identical flux distributions.

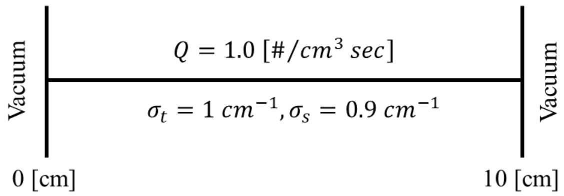

Fig. 2. Configuration of a fixed source slab problem.

Table 1. Number of iterations for convergence.

Methods	$p = 1$	$p = 2$
SI	143	
CMR	33	24
CMFD	22	33
pCMFD	14	24
One-node CMFD*	21	32
One-node CMFD	40	35
One-node pCMFD	41	35

One-node CMFD* represents two-node scheme application.

The number of transport sweep nodes was fixed at 10, hereafter referred to as local nodes. The number of local nodes per global node, denoted by p, was varied between 1 and 2. The resulting local node-wise flux distributions were identical for all cases. However, the number of iterations required for convergence differed depending on the acceleration scheme and was substantially reduced compared to the unaccelerated source iteration (SI) case. Convergence was determined when the L2 norm of the flux difference fell below 1E-9.

To further assess the numerical stability of each method, the slab length was extended to 1,000 cm, effectively approximating an infinite slab. Figures 3 to 5 present the computed numerical spectral radius for each method with $p = 4$ as the scattering cross section was varied. The overall trends are consistent with those reported in previous studies [7,9]. The numerical spectral radius was evaluated using the following expression

$$\rho_{num} = \frac{|\phi^{(l)} - \phi^{(l-1)}|}{|\phi^{(l-1)} - \phi^{(l-2)}|}, \quad (12)$$

where ϕ is the scalar flux and l is the iteration index.

As the scattering ratio $c = \sigma_s/\sigma_t$ increases, the stability of acceleration schemes generally deteriorates. For $c = 0.96$, only pCMFD and one-node pCMFD exhibit full convergence over the range of coarse-mesh optical thickness, defined as σhp, where σ denotes the total cross section, and h is the local node length.

In addition, one-node CMFD produces different numerical spectral radius ρ_{num} depending on whether it is implemented as a two-node scheme or in a parallel framework. The two-node implementation of one-node CMFD closely resembles the behavior of the conventional CMFD.

It should be noted that a higher numerical spectral radius ρ_{num} for one-node pCMFD does not necessarily imply a greater computational burden. Owing to the inherently parallel structure of the one-node formulation, true parallel execution can be achieved, which could effectively reduce the overall wall-clock time [5].

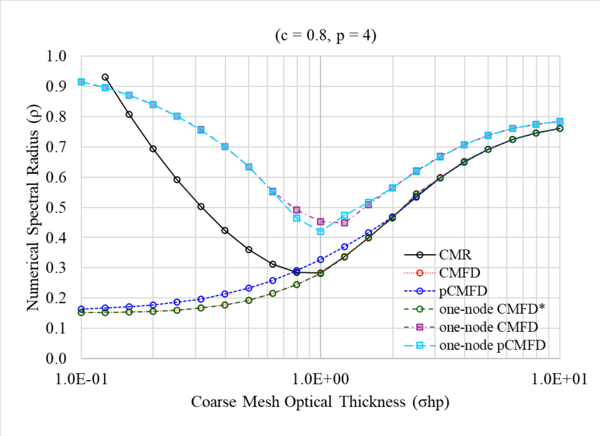

Fig. 3. Numerical spectral radius for $c = 0.8$ and $p = 4$.

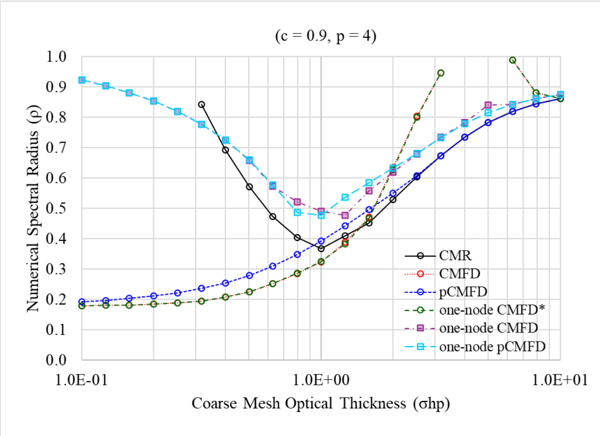

Fig. 4. Numerical spectral radius for $c = 0.9$ and $p = 4$.

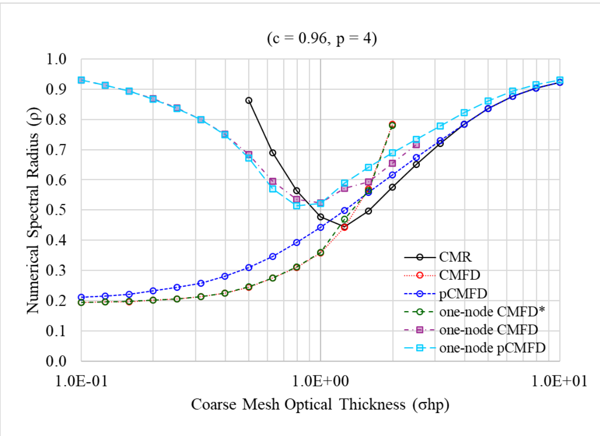

Fig. 5. Numerical spectral radius for $c = 0.96$ and $p = 4$.

Further analysis was conducted by varying the value of p. Figures 6 and 7 present the results for $c = 0.9$ with $p = 2$ and $p = 1$, respectively. For $p = 2$, all CMFD schemes except CMR converged. However, for $p = 1$, only one-node pCMFD achieved convergence over the entire domain, whereas conventional pCMFD did not.

These observations further confirm that pCMFD generally exhibits improved convergence characteristics. For fixed-source problems, the implementation form, whether two-node or parallel, can influence the convergence behavior, i.e., different ρ_{num} value.

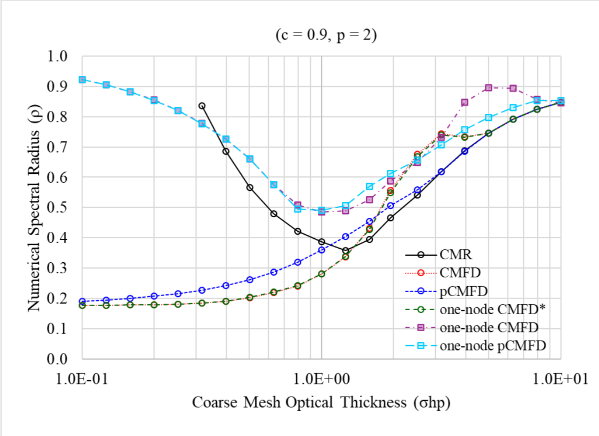

Fig. 6. Numerical spectral radius for $c = 0.9$ and $p = 2$.

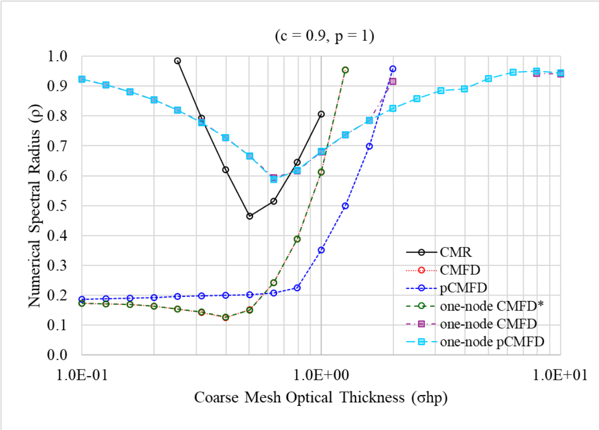

Fig. 7. Numerical spectral radius for $c = 0.9$ and $p = 1$.

The eigenvalue problem was formulated using the same one-group one-dimensional slab configuration, with the slab length set to 100 cm. Instead of an external fixed source, a fission source was introduced by assigning a fission cross section of $\nu\Sigma_f = 0.1\ \text{cm}^{-1}$. The scattering ratio was fixed at $c = 0.9$ with p value of 1.

Figure 8 presents the calculated spectral radius for the outer iteration in the eigenvalue problem. The spectral radius of the outer iteration was evaluated using the following definition [8].

$$\rho_{num} = \left[\frac{\left|\phi^{(l)} - \phi^{(l-1)}\right|}{\left|\phi^{2} - \phi^{1}\right|}\right]^{1/(l-2)}, \qquad (13)$$

In the fixed-source problem, the spectral radius is governed by the iterative scheme and differs noticeably between the parallel one-node implementation and the conventional two-node scheme. No such distinction is observed for the eigenvalue problem, where the spectral radius reflects the asymptotic convergence of the power iteration and is closely related to the dominance ratio. For example, the numerical spectral radius obtained for pCMFD and one-node pCMFD coincides over the range considered, as shown in Fig. 8. A similar independence from the implementation form is observed for one-node CMFD, in contrast to the fixed-source case.

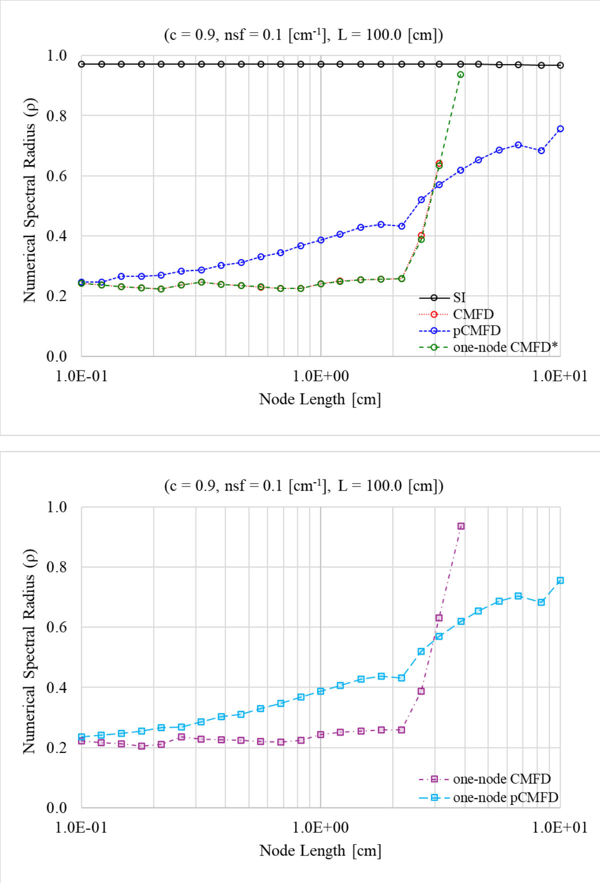

Fig. 8. Numerical spectral radius for eigenvalue problem.

It should be noted that the spectral radius of source iteration (SI) remains unchanged regardless of the computational node size [8]. Both conventional pCMFD and one-node pCMFD converge over the entire domain considered, whereas the other schemes do not. These results further confirm that pCMFD generally exhibits improved convergence characteristics for the eigenvalue problem as well.

4. Conclusions

This study compared the convergence behavior of several CMFD acceleration schemes for one-group one-dimensional slab neutron transport problems in both fixed-source and eigenvalue formulations under identical numerical conditions.

For the fixed-source problems, the convergence characteristics were influenced by both the CMFD formulation and the implementation structure. Differences were observed between two-node and parallel implementations of one-node CMFD. Among the schemes considered, pCMFD exhibited improved stability over a wide range of coarse-mesh optical thicknesses, and its one-node parallel implementation maintained convergence in cases where other schemes did not.

For eigenvalue problems, the convergence behavior was largely independent of the implementation form. The spectral radius associated with the outer iteration remained essentially identical between two-node and parallel one-node implementations. In this setting, both conventional pCMFD and one-node pCMFD converged over the entire domain considered.

Although one-node pCMFD may exhibit a relatively larger numerical spectral radius in certain fixed-source cases, its node-wise formulation enables true parallel execution, which can reduce wall-clock time despite the iteration count. These results indicate that pCMFD-based formulations provide stable convergence across problem types while offering practical advantages in parallel environments.

Future work will extend the present analysis to more general transport configurations and assess the performance of one-node pCMFD from a parallel scalability perspective.

ACKNOWLEDGMENTS

The authors would like to acknowledge Professor Nam Zin Cho for his broad and lasting contributions to the field of nuclear engineering and neutron transport theory. His work, including the development of partial-current CMFD, has had a continuing influence on subsequent research in this area.

REFERENCES

[1] K. S. Smith, "Nodal method storage reduction by nonlinear iteration", *Transactions of the American Nuclear Society* 44, 265. (1983)
[2] N.Z. Cho, G.S. Lee, C.J. Park, "On a New Acceleration Method for 3D Whole-Core Transport Calculations", Annual Meeting of the Atomic Energy Society of Japan (2003)
[3] H.C. Shin, Y. Kim. "A nonlinear combination of CMFD and FDFM methods", *Proceedings of Korean Nuclear Society Spring Meeting* (1999).
[4] Seongho Song, Hwanyeal Yu, Yonghee Kim, "One-node and two-node hybrid coarse-mesh finite difference algorithm for efficient pin-by-pin core calculation", Nuclear Engineering and Technology 50, 327-339 (2018).
[5] Jaeha Kim, Yonghee Kim, "Development of 3-D HCMFD algorithm for efficient pin-by-pin reactor analysis. Annals of Nucl Energy 127, 87-98 (2019).
[6] D. Wang, S. Xiao, "A Linear Prolongation Approach to Stabilizing CMFD". Nucl. Sci. Eng. 190, 45–55 (2018).
[7] N. Z. CHO and C. J. PARK, "A Comparison of Coarse Mesh Rebalance and Coarse Mesh Finite Difference Accelerations for the Neutron Transport Calculations," Proc. M&C 2003, Gatlinburg, Tennessee, April 6–11, 2003, American Nuclear Society (2003)
[8] Ser Gi Hong, Kang-Seog Kim, Jae Seung Song, "Fourier Convergence Analysis of the Rebalance Methods for Discrete Ordinates Transport Equations in Eigenvalue Problems", Nuclear Science and Engineering, 164:1, 33-52, (2010).
[9] Hyeon Tae Kim, Yonghee Kim, "Convergence Studies on Nonlinear Coarse-Mesh Finite Difference Accelerations for Neutron Transport Analysis", Nuclear Science and Engineering, (2018).
[10] Taesuk Oh, Yonghee Kim, "Investigation of Nodal Numerical Adjoints From CMFD Based Acceleration Methods", Front. Energy Res. 10:873731.
[11] E. E. Lewis, W. F. Miller, Jr., "Computational Methods of Neutron Transport", John Wiley & Sons, New York, 1984.